



# Selenium-functionalized polycarbonate-polyurethane for sustained *in situ* generation of therapeutic gas for blood-contacting materials

Peichuang Li<sup>a,b</sup>, Wanhao Cai<sup>a,c</sup>, Keping Wang<sup>a</sup>, Lei Zhou<sup>a</sup>, Shusheng Tang<sup>a</sup>, Yuancong Zhao<sup>a,\*</sup>, Xin Li<sup>a,d,\*\*</sup>, Jin Wang<sup>a,\*\*\*</sup>

<sup>a</sup> Key Laboratory of Advanced Technologies of Materials, Ministry of Education, School of Materials Science and Engineering, Southwest Jiaotong University, 610031, Chengdu, China

<sup>b</sup> Heze Branch, Qilu University of Technology (Shandong Academy of Sciences), Biological Engineering Technology Innovation Center of Shandong Province, Heze, 274000, China

<sup>c</sup> Institute of Physical Chemistry, Albert-Ludwigs-Universität Freiburg, Albertstr. 21, 79104, Freiburg, Germany

<sup>d</sup> Department of Cardiology, Third People's Hospital of Chengdu Affiliated to Southwest Jiaotong University, Chengdu, 610031, China

## ARTICLE INFO

### Keywords:

Selenium  
Polycarbonate-polyurethane  
Hemocompatibility  
Endothelialization  
Anti-hyperplasia

## ABSTRACT

Polyurethanes (PU) have been widely used in blood-contacting devices including indwelling implants and extracorporeal devices due to its good biocompatibility. However, the conventional PU also faces problems like thrombus formation and cell compatibility that could cause the treatment failure. In this study, a novel selenium-functionalized polycarbonate-polyurethane (PCU-SeSe) is developed based on the dynamic diselenide bond. Having diselenide bond-containing glycol as functional component, PCU-SeSe is endowed with glutathione peroxidase (GPx)-like catalytic activity, which could catalyze the release of nitric oxide (NO) continuously and controllably in the donor environment. This feature provides the materials with multiple functions from markedly suppressing platelet adhesion and activation, reducing the thrombogenesis, and enhancing the hemocompatibility. Meanwhile, PCU-SeSe could promote the growth of endothelial cell (EC) as well as significantly inhibit the growth of smooth muscle cell (SMC) and macrophage (MA) *in vitro*. The animal experiments including aortic implantation of sprague-dawley (SD) rats and stent implantation also demonstrate the abilities of endothelialization, thromboresistance, anti-inflammation, and anti-hyperplasia of PCU-SeSe *in vivo*. Overall, this study provides a new strategy for the designing of blood-contacting devices, which could be promising in the fabrication of cardiovascular biomaterials.

## 1. Introduction

Blood-contacting materials [1] have been widely used in the development of interventional devices and extracorporeal medical devices such as cardiovascular stent [2], arteriovenous grafts [3], artificial organs [4], and blood purification catheter [5]. However, the applications of the materials are strongly restricted by their side effects [1,6–8] like thrombus, inflammation and hyperplasia, which could threaten the lives of patients. To solve the problem, a variety of strategies have been developed for improving the properties of blood-contacting devices. For example, numerous methods including polymer coatings [9], polymer

brush [10], nanoparticle coating [11], biomolecule immobilization [12, 13], drug load or conjugate [14,15], and surface graphics [16] have been applied to ameliorate clinical complications of cardiovascular stents. Nevertheless, insufficient biocompatibility of the related polymer coating often results in unavoidable restenosis and thrombus [17]. Therefore, the update of the polymer coating and materials remains very urgent.

Polyurethanes (PU) as a valuable candidate has attracted more and more attention due to its excellent mechanical property and special structure, which also shows a low performance in biocompatibility [17, 18]. Consequently, numerous modifications (e.g., polymer grafting [19], small molecules grafting, peptide fixation [20], drug incorporation [21],

\* Corresponding author.

\*\* Corresponding author. Key Laboratory of Advanced Technologies of Materials, Ministry of Education, School of Materials Science and Engineering, Southwest Jiaotong University, 610031, Chengdu, China.

\*\*\* Corresponding author.

E-mail addresses: [zhaoyc7320@163.com](mailto:zhaoyc7320@163.com) (Y. Zhao), [Lixin131715@163.com](mailto:Lixin131715@163.com) (X. Li), [wangjin@swjtu.edu.cn](mailto:wangjin@swjtu.edu.cn) (J. Wang).

<https://doi.org/10.1016/j.smaim.2022.04.003>

Received 13 April 2022; Received in revised form 29 April 2022; Accepted 29 April 2022

Available online 4 May 2022

2590-1834/© 2022 The Authors. Publishing services by Elsevier B.V. on behalf of KeAi Communications Co. Ltd. This is an open access article under the CC BY-NC-ND license (<http://creativecommons.org/licenses/by-nc-nd/4.0/>).

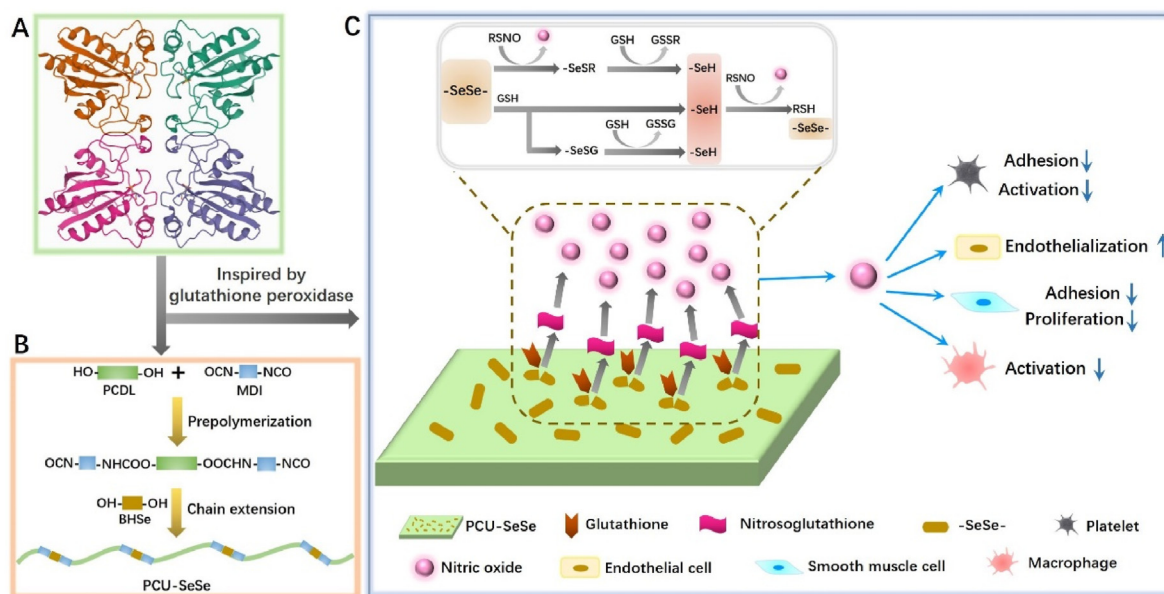


**Fig. 1.** (A) Inspired by glutathione peroxidase, (B) selenium-functionalized polymer PCU-SeSe was synthesized by two-step polymerization. (C) The sustained *in situ* generation of NO endows the PCU-SeSe with multi-functions in blood environment, leading to the enhancement of anti-coagulant, anti-inflammatory, anti-hyperplastic, as well as the promotion of endothelial properties.

and nitric oxide (NO) donor load [22]) have been proposed to prepare high-performance PU. However, most of the modifications can hardly achieve multiple functions. For instance, the grafting of the anti-fouling component is an effective strategy in the inhibition of thrombosis, but on contrary, will result in the delay of tissue healing due to the resistance of cell adhesion [23]. Drug incorporation as another strategy could also effectively inhibit thrombosis and reduce the inflammation in the early implantation stage, but will lead to a high risk of restenosis and thrombosis in the late stage [24]. Thereout, the multiple functions of blood-contacting PU are strongly preferred. Moreover, PU can obtain special properties by adjusting the type of raw materials. Hence, synthetic approach may be feasible for blood-contacting PU to meet the complex requirements of blood environment.

The problems may be solved by introducing NO into the system. The biosynthesis of NO within endothelial cells (EC) and endogenous S-nitrosothiols (RSNO) in blood could effectively prevent the formation of thrombosis [25,26]. It could inhibit not only the adhesion of platelets, but also the proliferation of smooth muscle cell (SMC). At the same time, it promotes the proliferation of vascular endothelial cell, hence providing a normal vascular environment [27]. Notably, endothelium release NO was under the action of endothelial nitric oxide synthase (eNOS). However, the eNOS activity is impaired at the diseased site [28]. The exogenous NO provided by NO-releasing materials can hardly be provided in the long term [29,30]. The optimizing strategy could be by using endogenous RSNO to produce NO in the vascular system [30–32]. Inspired from glutathione peroxidase (GPx) in the blood, organoselenium moieties were found to have the function to decompose RSNO to generate NO at local material interfaces by catalyzing the transformation between Se–Se and Se–S bonds [33], while the reversibility of Se–Se bond can be realized by dynamic chemistry. Although there were other dynamic bonds (e.g., disulfide bond) be used to catalyze the release of NO, the kinetics of disulfide metathesis was very slow due to the high bond energy and apparent activation energy [34]. In comparison, the NO release levels of diselenide bonds are similar to normal endothelial cells due to the lower bond energy (172 kJ/mol), hence could be easily achieved. Since GPx-like catalyzing can ensure a continuous NO release *via* mobilizing regenerative endogenous RSNO, it may be feasible to use selenium-containing materials in the design of the blood-contacting polyurethane materials for the vascular implants.

In this study, we proposed a promising strategy to develop novel blood-contacting polycarbonate-polyurethane (PCU) materials *via* selenium element. Inspired by endogenous biochemical reactions in the human body involving GPx mimics catalytic capability, selenium-containing diols (BHSe) [35] as chain extenders were introduced into PCU molecule with a simple solvent polymerization method. As shown in Fig. 1, this avenue endows this novel PCU material with excellent capability to continuously and controllably produce NO based on dynamic chemistry. To evaluate the biological properties of the obtained materials, various blood tests including platelet adhesion and blood circulation were first performed to explore the blood compatibility. Moreover, the main blood vessel cells including EC, SMC and macrophage (MA) were cultured on the samples surface to explore cell compatibility. A series of animal experiments including subcutaneous embedding, aortic implantation and stent implantation were used to assay the *in vivo* biocompatibility.

## 2. Materials and methods

### 2.1. Materials and reagents

Selenium powder was purchased from Aladdin Chemical Reagent Co. Ltd. (Shanghai, China). 2-bromoethanol was purchased from TCI. Diphenylmethane-4,4'-diisocyanate (MDI), stannous octoate, S-nitrosoglutathione (GSNO), and L-glutathione (GSH) were all purchased from Sigma-Aldrich. Polycarbonatediol (PCDL) was purchased from UBE industries, LTD. 1,4-Butylene glycol (BDO) and N,N-Dimethylacetamide (DMAc) were dried under vacuum before use.

### 2.2. Synthesis of bis(2-hydroxyethyl) diselenide and PCU-SeSe

First, 3.18 g of selenium powder (40.2 mmol) was added into a 250 mL flask containing 40 mL aqueous solution of sodium borohydride (1.52 g, 40.0 mmol). Then the mixture was stirred in an ice bath for 10 minutes under argon atmosphere, and for 20 minutes under room temperature respectively, followed by warmed briefly on the steam bath to obtain the brownish red aqueous solution of Na<sub>2</sub>Se<sub>2</sub>. Then, 80 mL of THF solution containing 5.03 g of 2-bromoethanol was injected into the Na<sub>2</sub>Se<sub>2</sub> solution with stirring at 50 °C for 6 h under argon atmosphere.

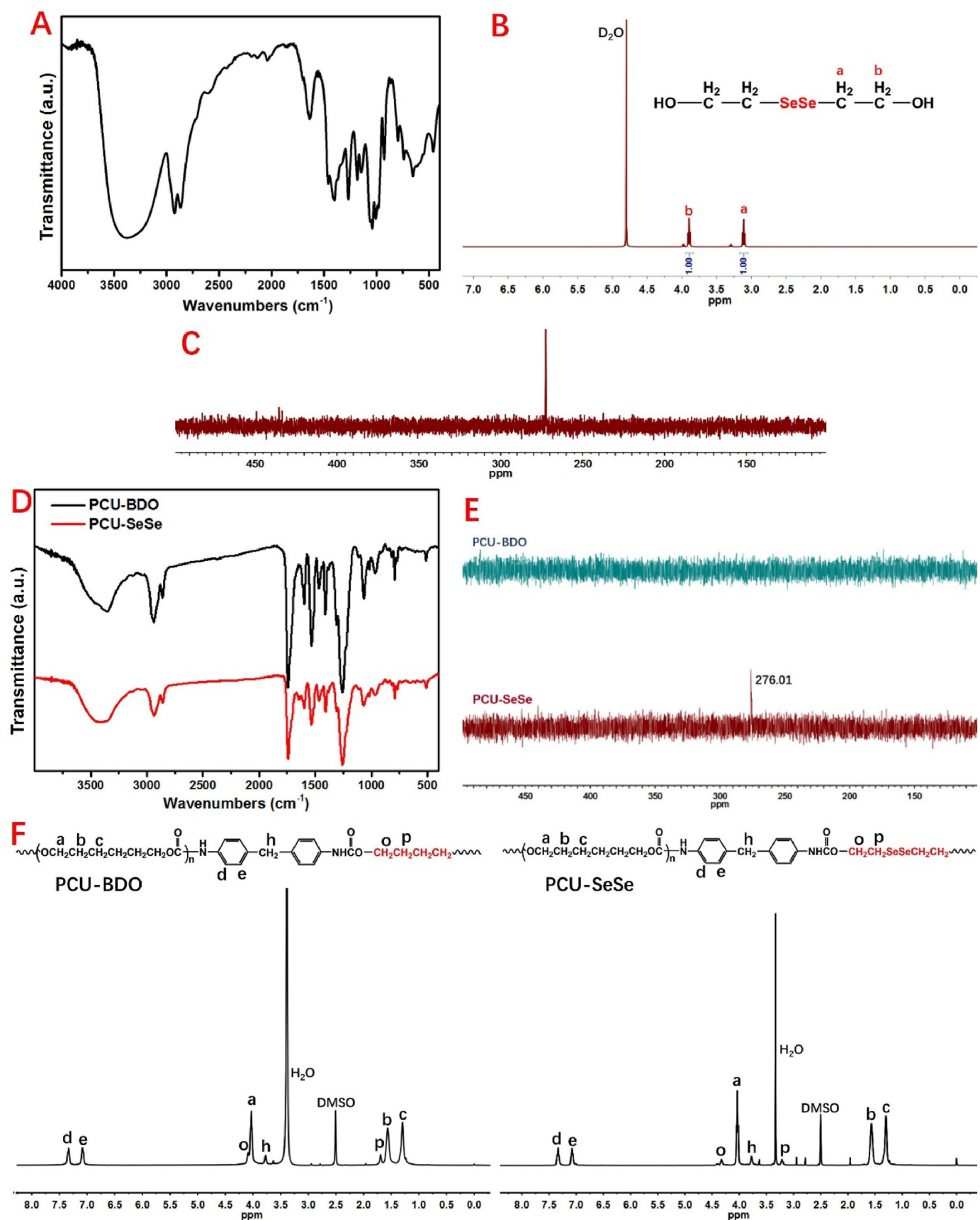
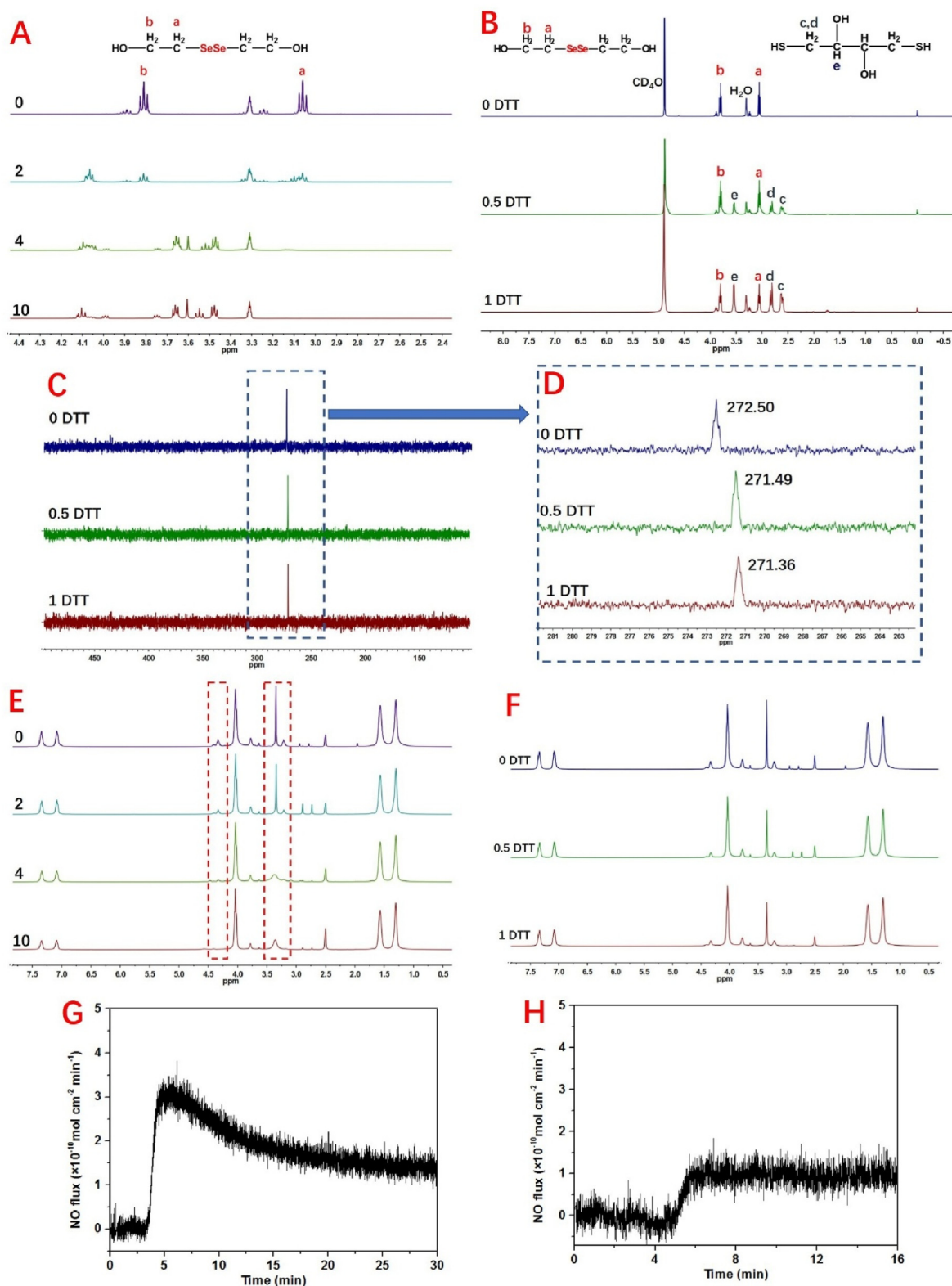


Fig. 2. Structural analysis of BHSe including (A) FTIR, (B) <sup>1</sup>H NMR, and (C) <sup>77</sup>Se NMR spectra; Structural analysis of PCU-BDO and PCU-SeSe including (D) FTIR, (E) <sup>77</sup>Se NMR and (F) <sup>1</sup>H NMR spectra.



**Fig. 3.** Redox response and NO release. The amount of  $\text{H}_2\text{O}_2$  and DTT are both relative to the total number of diselenide bonds in reactants (i.e. BHSe or PCU-SeSe). (A)  $^1\text{H}$  NMR results of BHSe reacting with different equivalent  $\text{H}_2\text{O}_2$ . (B)  $^1\text{H}$  NMR spectra and (C)  $^{77}\text{Se}$  NMR analysis of BHSe reacting with DTT. (D) Partial enlargement of Fig. 3C. (E)  $^1\text{H}$  NMR results of PCU-SeSe reacting with different equivalent  $\text{H}_2\text{O}_2$  and (F) DTT. (G) NO release curves of PCU-SeSe before and (H) after 30 days.

After the termination of the reaction, 50 mL of ethyl acetate was added into the final reaction mixture and the product was extracted into the organic layer [35]. The organic layer was dried then with anhydrous  $\text{Mg}_2\text{SO}_4$  and concentrated under vacuum, followed immediately by

purified by column chromatography using an eluent of dichloromethane and ethyl acetate (v/v, 1:1.1). Finally, bis(2-hydroxyethyl) diselenide (BHSe) was successfully synthesized (Yield: 51%, see Fig. S1A in supplementary materials for synthesis route).

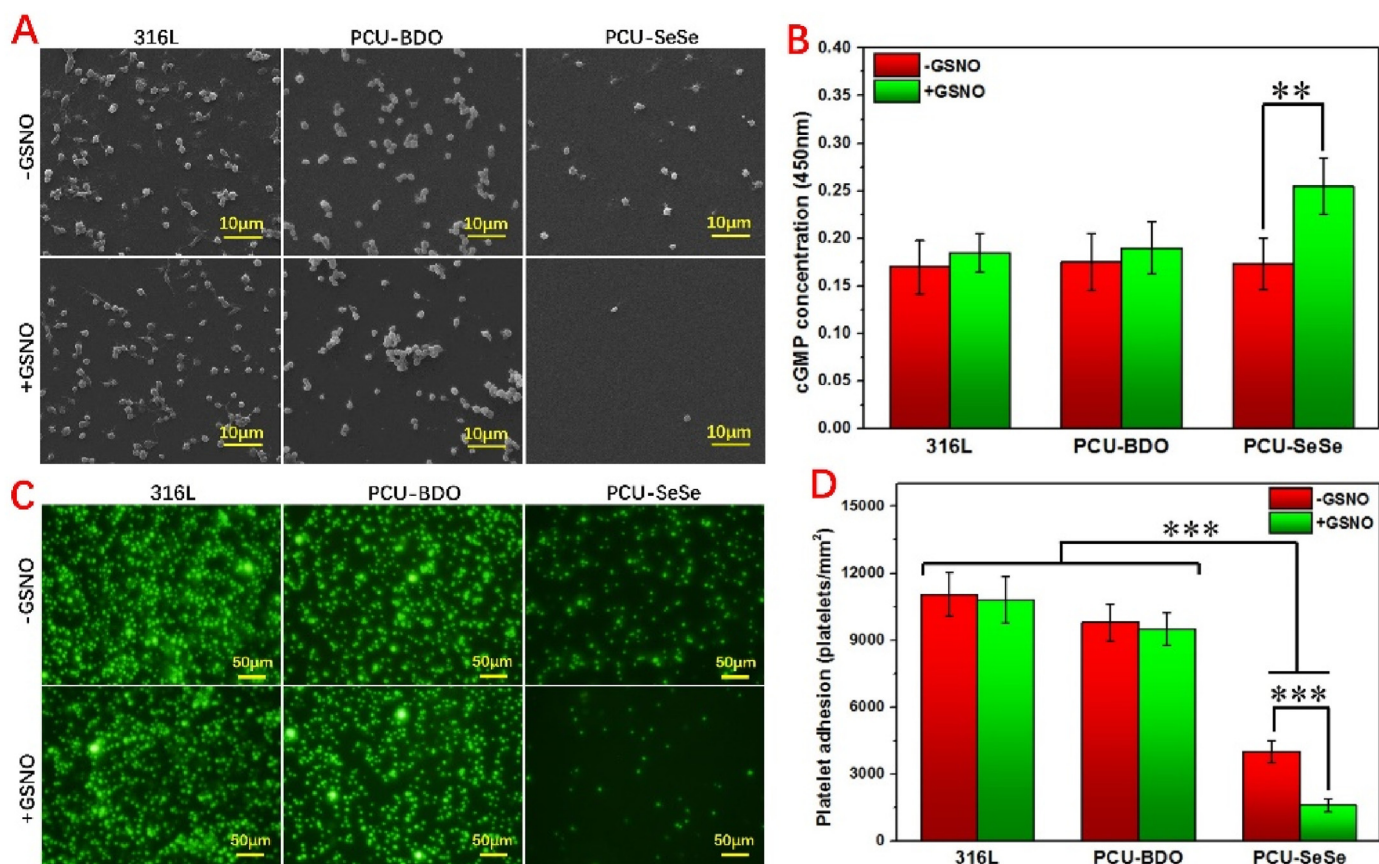


**Fig. 4.** Results of platelets interacting with different samples. (A) SEM images, (B) cGMP detection, (C) fluorescent images, and (D) statistical analysis of platelets on the surface of 316L, PCU-BDO and PCU-SeSe.

Referring to the principle of stepwise polymerization and our previous studies [23], PCU-SeSe was synthesized for the first time in this study according to the synthesis route (see Fig. S1B in supplementary materials). First of all, PCDL was heated to molten state and thoroughly dried under vacuum at 80 °C for further use. Then, moderate PCDL and MDI were added into a three-neck flask under argon atmosphere. Subsequently, DMAc as solvent was injected into flask and the reaction lasted for 2 h at 60 °C. After the prepolymer was obtained, DMAc containing chain extender i.e. BHSe was injected into flask. Besides, stannous octoate (0.1%) was added to facilitate the reaction process. After that, the reaction was allowed to continue at 60 °C for 6 h. Particularly, the feed ratio of MDI/PCDL/BHSe is 2/1/1 and the PCU-BDO was selected as the control sample. After chain extension, the final product was precipitated from the reaction solution. The resulting products were then thoroughly washed with ethanol and deionized water, respectively, then stored in a vacuum drying oven for further use.

### 2.3. Chemical composition and responsiveness of BHSe and PCU-SeSe

The chemical composition of BHSe was identified using Fourier transform infrared spectrometer (FTIR, NICOLET 5700) and nuclear magnetic resonance spectrometer (NMR, Bruker AV II-400) respectively. The molecular weight of BHSe was detected on a LCMS-IT-TOF apparatus using electrospray ionization mass spectrometry (ESI-MS) spectrum. Similarly, the structure of PCU-SeSe was proved by using FTIR, <sup>1</sup>H NMR and <sup>77</sup>Se NMR.

The responsiveness including reduction and oxidation reactions of BHSe and PCU-SeSe were validated by a series of NMR experiments. The diselenide bond content in BHSe or PCU-SeSe was first set to one equivalent. For the evaluation of reductive and oxidation responsiveness respectively, different respective equivalents of dithiothreitol (DTT) and

hydrogen peroxide (H<sub>2</sub>O<sub>2</sub>) were used to react with BHSe and PCU-SeSe, then analyzed using <sup>1</sup>H NMR and <sup>77</sup>Se NMR.

### 2.4. Preparation and hydrophilic detection of PCU-SeSe coated surface

As a common medical metal, 316L stainless steel (316L) sheet (diameter = 10 mm) was selected as the substrate of PCU-SeSe coating. Polytetrafluoroethylene (PTFE) mold and solvent evaporation were used for the preparation of the coating. First of all, 316L sheets were processed with polishing cloth to obtain the mirror-polished surface. Then, all sheets were ultrasonically cleaned three times by acetone, ethanol, and deionized water in sequence. After that, 316L sheets were dried and then placed in PTFE mold. PCU-SeSe solution (10%) was preliminarily prepared using tetrahydrofuran (THF) and then be poured into the PTFE mold. When the solvent volatilization is complete, PCU-SeSe coating was prepared and covered on the surface of 316L sheets. PCU-BDO coating was also obtained refer to the above method. 316L sheet without coating was used as a control in subsequent experiments. The hydrophilicity of samples was evaluated via water contact angle using a DSA100 Drop Shape Analyzer. During detection, a droplet of ultrapure water was placed on the sample surface, and then the water contact angle was determined and recorded using a horizontal microscope.

### 2.5. NO release evaluation

Real-time catalytic release of NO induced by PCU-SeSe sample was monitored by a chemiluminescence-based NO analyzer (NOA 280i). The PCU-SeSe sample was cast into 0.3 cm × 0.7 cm plate before the NO release experiment. First, 5 mL phosphate buffered saline (PBS, pH = 7.4) solution was added into the reaction vessel. Then, 10 μM GSNO and 10 μM GSH were added into the above solution as NO donor. Subsequently,

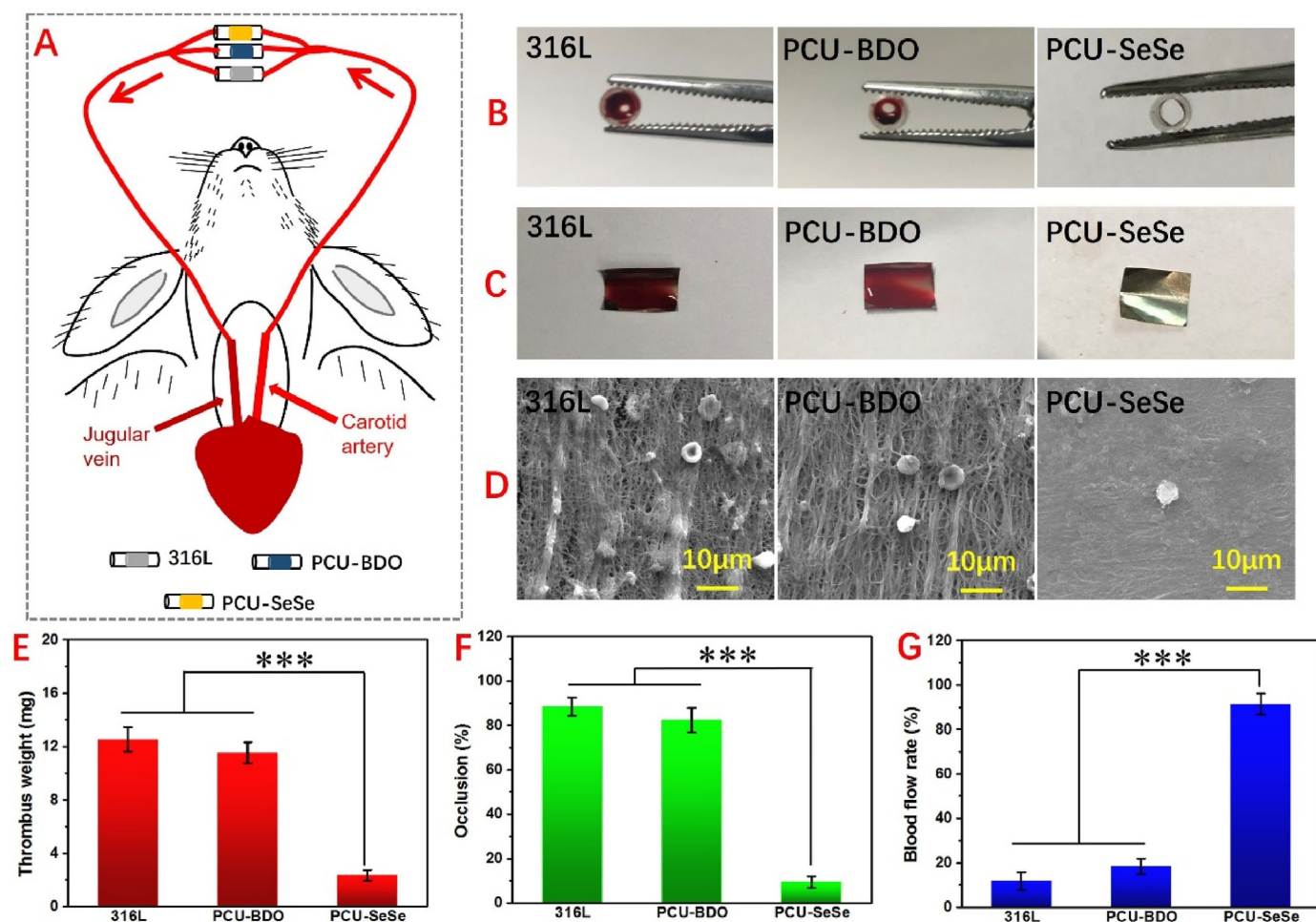


**Fig. 5.** Dynamic evaluation of the hemocompatibility of the PCU-SeSe in an arteriovenous shunt model of rabbits. (A) Sketch map of the experiment model. (B) Digital photos of cross-section and (C) thrombi after circulation. (D) SEM images and (E) thrombus weight on the sample surface. (F) Occlusion ratio of sample containing catheter by measuring the cross-section diameter of the blood circulation tube. (G) Relative blood flow rate at the end of circulation (compared with that of the initial blood flow).

the reaction vessel was protected from light and carried out with high purity nitrogen gas stream at 37 °C. After the baseline was collected and became horizontal, the PCU-SeSe sample was immersed into the solution and the signal of NO release was recorded by a computer. Finally, the amount of NO releasing was calculated and over three samples per group were checked.

## 2.6. Hemocompatibility evaluation

### 2.6.1. Platelet adhesion assay and cyclic guanosine monophosphate (cGMP) test

The acquisition and use of human blood were approved by Ethics and Welfare Committee of Southwest Jiaotong University and in accordance with the Laboratory Administration Rules. First, fresh human whole-blood was centrifuged at 1500 rpm for 15 minutes to obtain the platelet rich plasma (PRP). Particularly, 10 µM GSNO and 10 µM GSH were added into the PRP for the analysis of the NO effects on platelet adhesion and activation. Then, the same amount of PRP was dropped immediately onto each surface of samples and incubated at 37 °C for 1 h. Further, the samples were rinsed with PBS three times to remove non-firmly adsorbent platelets, then were fixed with 2.5 wt% glutaraldehyde solution overnight. After that, all the samples were respectively dehydrated, dealcoholized and critical point drying. Finally, the samples were gold sputtered and then observed via scanning electron microscopy (SEM) to evaluate the morphology and quantity of adherent platelets.

The cGMP concentration in the platelets which reacted with samples

was detected via a human cGMP enzyme-linked immunoassay kit (Hufeng Biotechnical Co., China). The samples were placed into a 24 well cell culture plate and 400 µL PRP was added onto the samples. Particularly, 20 µM GSNO and 20 µM GSH were added into the donor-containing group for comparative analysis. After incubation at 37 °C for 30 minutes, 10% Triton-X was added into the reaction solution and then platelet membranes were ruptured using sonication for 10 minutes. After that, the solution was centrifuged at 2500 rpm for 10 minutes to obtain the supernatant. Finally, the supernatant was used to test the cGMP concentration via enzyme linked immunosorbent assay (ELISA) kits according to the manufacturer instructions.

### 2.6.2. Ex vivo blood circulation

In this study, all animals were raised in a standard animal house (Basic Animal Laboratory, West China Medical College) according to the relevant requirements of experimental animal breeding. Moreover, all procedures for animal experiment were approved by the Animal Care and Use Committee of Southwest Jiaotong University and complied with the Guide for the Care and Use of Laboratory Animal of the National Institutes of Health (NIH). The *ex vivo* blood circulation was conducted using adult New Zealand white rabbits weighing ~4 kg each. All of the experimentation on animals was abided by the Local Ethical Committee and Laboratory Animal Administration Rules of China following the ethical rules. First, the PCU-TeTe coating was prepared on the surface of 316L foils (~8 mm × 10 mm) via solvent evaporation. Then, the foils were rolled up and placed into the cardiopulmonary perfusion catheters.

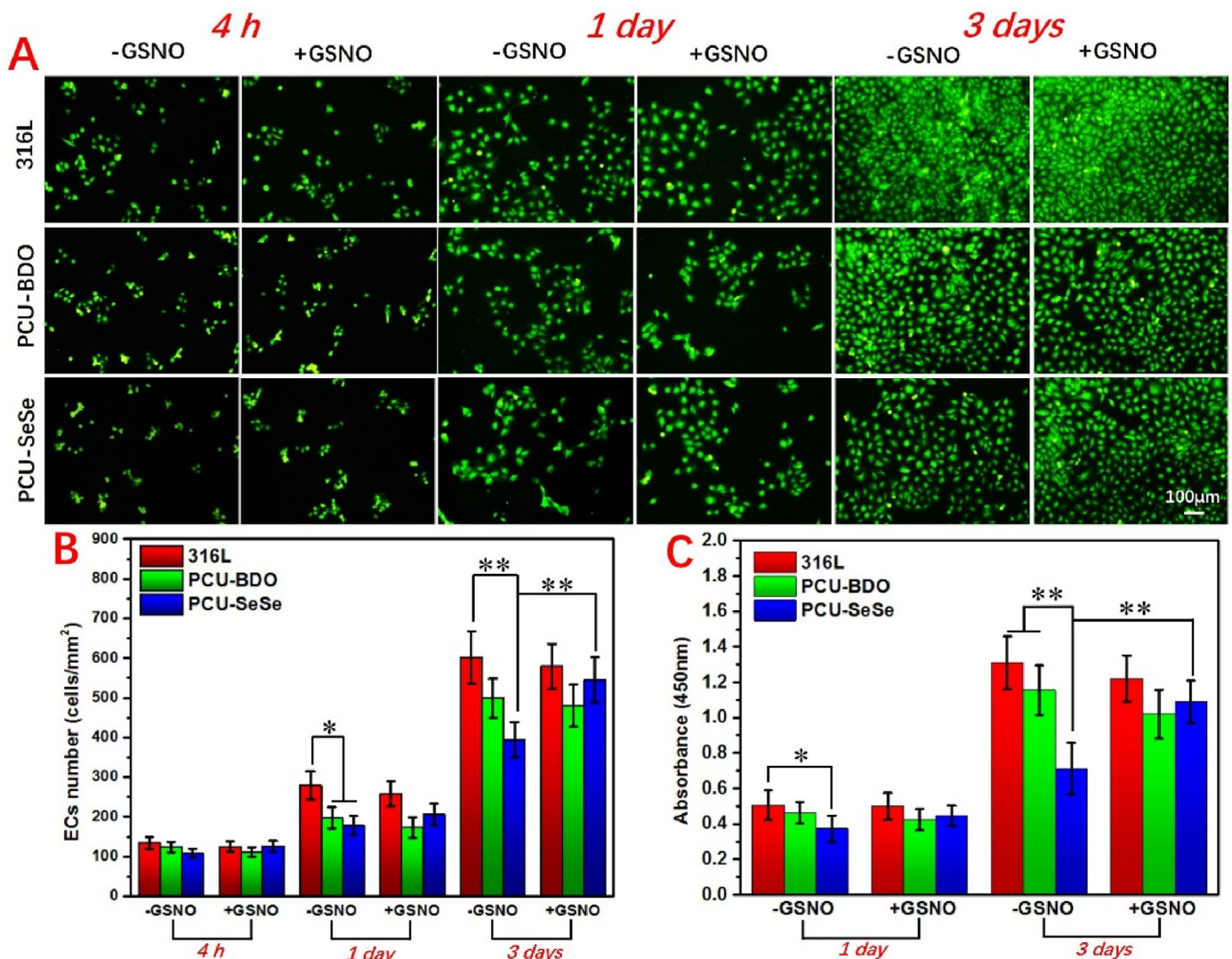


Fig. 6. (A) Cal-AM staining of EC. (B) Statistical analysis of cell number and (C) vitality.

After the exposure of different sides of carotid artery and jugular vein, one surgical indwelling needle was connected with carotid artery and the other indwelling needle were connected with jugular vein. Immediately, perfusion catheters containing samples were linked with the indwelling needles to construct *ex vivo* circulation loop. Meanwhile, considering the limited endogenous NO donor of rabbits, GSNO (10 mM) and GSH (10 mM) were injected into the rabbit through ear vein. The catheter around the sample was cut off after 1 h of *ex vivo* blood circulation, after which the cross section and the clot on the sample surface were photographed. Subsequently, the thrombus formed on the samples surface were respectively fixed with glutaraldehyde (2.5 wt%), dehydrated, dealcoholized and weighed. Finally, thrombus microtopography of different samples was observed by SEM.

## 2.7. Cytocompatibility

### 2.7.1. EC culture

Vascular EC in this study was cultured in M199 (Hyclone) medium added with 15% fetal bovine serum (FBS) refer to the previous study [36]. The samples were immersed in 1 mL culture medium containing  $1.5 \times 10^4$  EC and then moved in an incubator (37 °C, 5% CO<sub>2</sub>). During culture process, 10 μM GSNO and 10 μM GSH were supplemented in donor-containing groups every 24 h. At the predetermined time (4 h, 1 day and 3 days), calcein-AM (Cal-AM, 4 μg/mL) as fluorochrome was

added into medium to stain the cells on the samples surface. After cleaning with PBS and fixing with glutaraldehyde, stained samples were observed via fluorescent microscope (IX51, Olympus). Besides, cell counting kit-8 (CCK-8, Dojindo) was used to analyze the EC viability.

### 2.7.2. SMC growth

As the previous description, artery SMC was cultured in a medium consisting of 85% Dulbecco's modified Eagle medium/F12 (Hyclone) and 15% FBS. Each sample was soaked in 1 mL medium containing  $2.0 \times 10^4$  SMC. The subsequent processes were similar to that of EC culture, GSNO and GSH were added in donor-containing groups. After the predetermined time, fluorescent microscope was used to observe SMC growth status and CCK-8 was used to detect SMC viability. Moreover, human cGMP enzyme-linked immunoassay kit was used to analyze the cGMP levels of SMC after 45 min culture.

### 2.7.3. MA culture

Mouse mononuclear macrophages (RAW 246.7) were seeded on the samples with a density of  $5.0 \times 10^4$  cells/sample and NO donors were chosen as control variable. MA culture medium consisting of 85% High Gly medium (Hyclone) and 15% FBS. MA culture was performed for different time intervals (4 h, 1 day and 3 days) using an incubator at 37 °C. After culture, the samples were stained with Cal-AM and then fixed with glutaraldehyde (2.5%) for 12 h. Next, fluorescence microscope

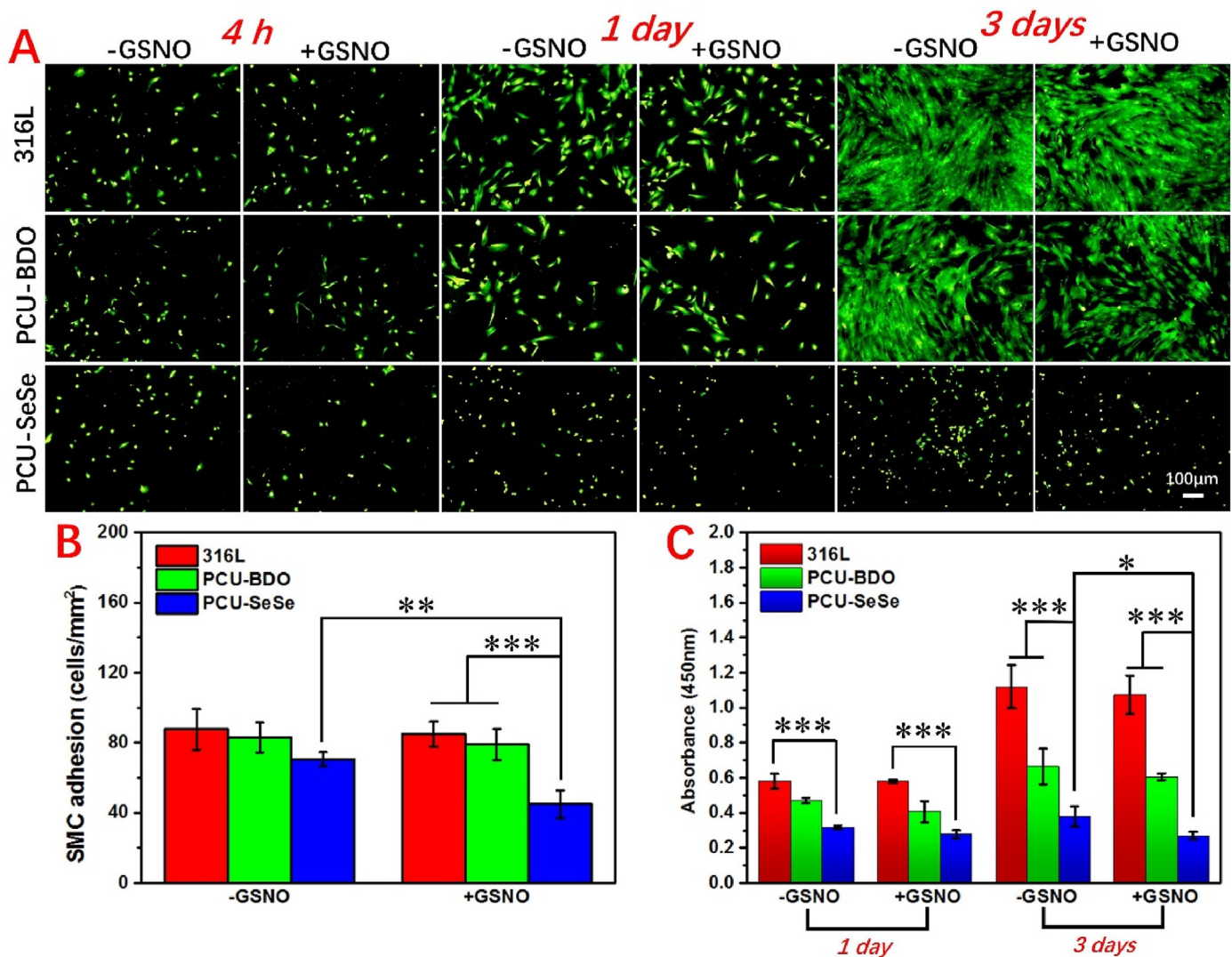


Fig. 7. (A) Cal-AM staining, (B) 4 h count, and (C) CCK-8 results of SMC on the samples surface.

(Zeiss) was used to observe the growth status of MA at different time points. Subsequently, ELISA kits including interleukin-6 (IL-6) and tumor necrosis factor (TNF- $\alpha$ ) were used to analyze the 3 days of MA culture medium. The contents of IL-6 and TNF- $\alpha$  in the medium were detected to investigate the anti-inflammatory levels of the samples.

## 2.8. Implantation experiments

In this section, a series of animal experiments including subcutaneous embedding, aortic implantation and stent implantation were used to evaluate the *in vivo* biological behaviors. Particularly, all procedures for animal experiments were approved by the Animal Care and Use Committee of Southwest Jiaotong University and complied with the Guide for the Care and Use of Laboratory Animal of the National Institutes of Health (NIH).

### 2.8.1. Subcutaneous embedding

The subcutaneous embedding model was constructed by implanting the samples under the back skin of male Sprague Dawley (SD) rats ( $n = 12$ , approximately 300 g). Two time points including 3 weeks and 9 weeks were set to explore the short-term and long-term subcutaneous behavior of different samples. At the appointed time, fibrous tissues that formed around different samples were collected and then cleaned with PBS. Immediately, all the samples were immersed into paraformaldehyde

at 4 °C for 3 days. After that, fixed samples were required to ethanol-dehydrated and xylene-saturated. Subsequently, the samples were embedded in paraffin and then sliced with slicer. At last, obtained tissue samples were stained with hematoxylin and eosin (HE) and then pictured via optical microscope.

### 2.8.2. Wire implantation

Twelve Healthy adult SD rats (male, approximately 300 g) were used in the aortic implantation [37]. The PCU-SeSe was sprayed onto the 316L wires. Six rats were used for the uncoated wires (316L) and the other six were used for the coated wires (PCU-SeSe). Before implantation, the rats were given general anesthesia by injection of pentobarbital sodium (3%). Next, rat abdominal aortas were isolated and then injected with heparin solution for anticoagulation during wire implantation. Immediately, the vascular wounds were sewn up and wires were attached to the vessel. After that, intraperitoneal anti-inflammatory treatment was performed with gentamicin (2 mL,  $0.2 \times 10^5$  U/mL). After skin suture, the wounds were swabbed with iodophor and then penicillin (1 mL,  $1.0 \times 10^5$  U/mL) was injected into the muscles of rats. After 30 days of feeding, the blood vessels containing the samples were collected and then rinsed with heparinized saline carefully. Subsequently, the obtained samples were soaked with paraformaldehyde, observed with SEM, and stained with immunofluorescence successively.

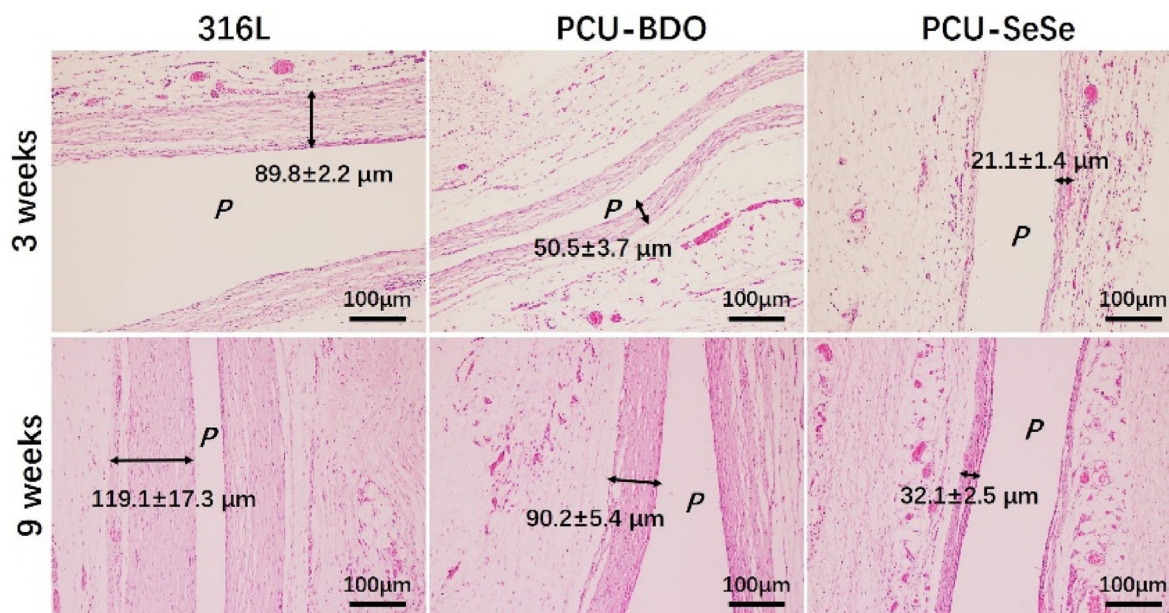


Fig. 8. HE staining of fibrous capsules around different samples (*P* represents the implantation location and the thickness of the fibrosis correlates with the level of inflammation).

### 2.8.3. Stent intervention

For stent intervention, adult New Zealand white rabbits (approximately 3 kg,  $n = 3$ ) were chosen as model animals [7,14,36]. All rabbits were raised in a standard animal house. Prior to the intervention, all the stents that needed to be implanted along with the balloon catheter were compressed via a stent crimper. Then, the rabbits were given pentobarbital sodium intravenously for general anesthesia. Subsequently, PCU-SeSe coated stents and bare stents were severally implanted into the left and right iliac arteries via percutaneous vascular balloon. After that, the animals were fed with warfarin sodium (0.6 mg, dissolved in water) and injected with penicillin (1 mL,  $1.0 \times 10^5$  U/mL) within the first 3 days of intervention. In the following 27 days, regular feeding was performed on the postoperative rabbits. Whereafter, the vessels containing the stents were collected and then fixed in glutaraldehyde solution. Then, the stents were cut evenly into two sections. One section was dissected longitudinally and photographed using SEM, the other was used for hard tissue embedding. Finally, the plexiglass fixed samples were sliced into thin layers and then recorded via microscope.

### 2.9. Statistical analysis

All the statistical values were presented as mean  $\pm$  standard deviation. Statistical significance was evaluated by one-way analysis of variance (ANOVA) and the statistical significance was set at  $P < 0.05$ .

## 3. Results and discussion

### 3.1. Structure of BHSe and PCU-SeSe

The successful synthesis of the BHSe was validated by several different methods. Fig. 2A shows the FTIR spectrum with typical peaks at 3375, 2924 and 2987  $\text{cm}^{-1}$ . The former peak can be assigned to the hydroxyl group, while the last two peaks belong to the methylene group. Fig. 2B shows the  $^1\text{H}$ -NMR spectrum with  $\text{D}_2\text{O}$  as the solvent. The chemical shift values at 3.11 ppm and 3.90 ppm corresponds to the  $-\text{CH}_2$  group of BHSe. Fig. 2C shows the  $^{77}\text{Se}$ -NMR spectrum, a clear chemical shift at 272.5 ppm is ascribed to the diselenide bond [38,39]. All these spectra results indicate the successful synthesis of BHSe. This conclusion is further supported by the molecular weight ( $M_w$ ) analysis. As shown in Supplementary Fig. S2, the negative ion mode of ESI-MS shows a  $M_w$  of

248.9598, in good agreement with the theoretical prediction (249.9011) minus a proton.

Similar to the BHSe, the product of PCU-SeSe and PCU-BDO were also analyzed by different methods. As the FTIR results are shown in Fig. 2D, the peak of isocyanate group vanishes in the FTIR, indicating that isocyanate in MDI is reacted completely. By contrary, the peaks of methylene (2924 and 2867  $\text{cm}^{-1}$ ) and benzene ring of MDI at 1598  $\text{cm}^{-1}$  are clearly observed. In the  $^{77}\text{Se}$ -NMR spectra (Fig. 2E), the only peak at 276.01 ppm is ascribed to the Se–Se of PCU-SeSe [38,39]. In the  $^1\text{H}$ -NMR spectra (Fig. 2F), the methylene groups of BDO and PCU-BDO can be observed at 4.09 and 1.69 ppm respectively. All these spectra results reveal the successful synthesis of the PCU-SeSe and PCU-BDO.

### 3.2. Redox response and NO release

Next, the redox response of BHSe and PCU-SeSe were validated by a series of NMR experiments [38,39]. Firstly, the oxidation response of BHSe reacted with different equivalent  $\text{H}_2\text{O}_2$  are monitored by the  $^1\text{H}$  NMR (Fig. 3A). It is found that the absorption peak intensity of methylene decreases with the increasing of  $\text{H}_2\text{O}_2$ : the absorption peak decreases remarkably under the action of 2 equivalent  $\text{H}_2\text{O}_2$ , while it vanishes until enough  $\text{H}_2\text{O}_2$  (4 and 10 equivalent) are applied, indicating that the diselenide bonds were completely oxidized and dissociated. These results indicated that the diselenide bonds can directly react with oxygen atoms and be dissociated in oxidizing medium, which endows PCU-SeSe with anti-inflammatory ability.

Then, the reduction response of BHSe was monitored by reacting with different dithiothreitol (DTT). In the  $^1\text{H}$  NMR spectra (Fig. 3B), the proton resonances of BHSe remains unchanged. Meanwhile, in the  $^{77}\text{Se}$  NMR (Fig. 3C), the chemical shift of diselenide bonds is almost constant at around 272 ppm (Fig. 3D) with slight shift, which only associates with the effects of DTT in the test solution. Similar oxidation and reduction responses (Fig. 3E and F) can be also observed for PCU-SeSe. These results indicate that the diselenide bond could be easily recovered after treating with DTT. That is, the dynamic diselenide bond breaking and healing can be realized in the reduction environment. This feature will then dominate the continuous catalytic release of NO (Fig. 1C), as confirmed in the section of NO release of PCU-SeSe.

Similar to the structure of GPx, diselenide bond in PCU-SeSe has the ability to decompose endogenous NO donors and release NO. The

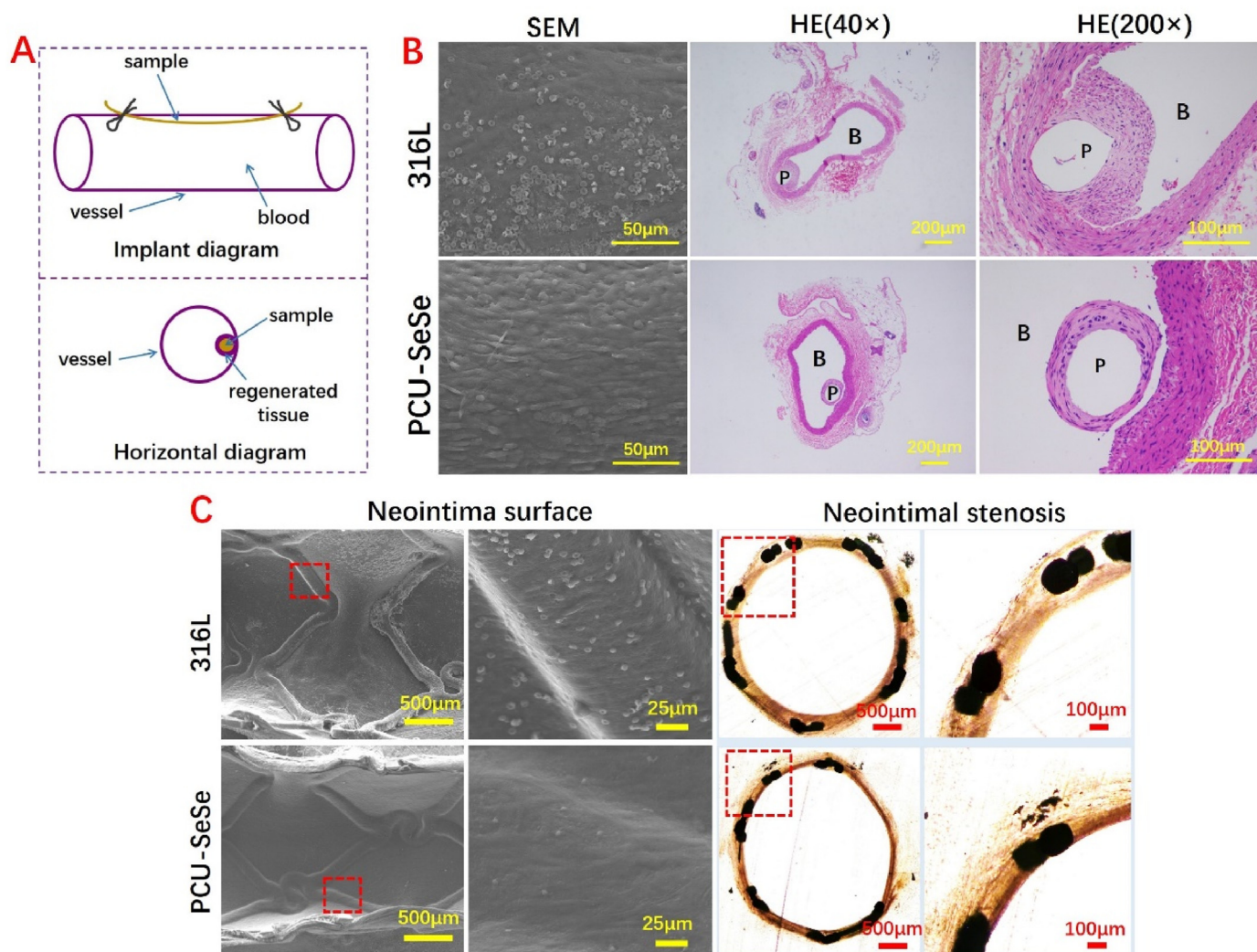


**Fig. 9.** Bare metal samples before and after modification were implanted into abdominal aortas of SD rats for 30 days. (A) Schematic diagram of the location of sample implantation and regenerative tissue. (B) SEM images of regenerative tissue surface and HE staining of tissue sections (B and P represent blood flow and sample sites, respectively); Stent implantation results of iliac artery in New Zealand rabbits. (C) SEM images of the neointima surface and histological pictures of the neointima stenosis.

catalytic capacity of PCU-SeSe was detected by chemiluminescence [26, 36], as shown in Fig. 3G. It can be seen that the NO release increases rapidly after the addition of sample into the donor solution. Then, the curve decreases slowly and stabilizes at the release platform of  $1.45 \times 10^{-10} \text{ mol cm}^{-2} \cdot \text{min}^{-1}$ , reaching the normal NO release level of EC. In such process, part of NO was produced from the direct decomposition of NO donor by diselenide bonds, and the rest came from multistage reactions between diselenide bonds and GSH and NO donor. Subsequently, the test samples were transferred into a vacuum oven. After 30 days, the stored samples were tested again for NO release rate. As shown in Fig. 3H, a significant catalytic rate ( $1.05 \times 10^{-10} \text{ mol cm}^{-2} \times \text{min}^{-1}$ ) can still be observed in the NO release from PCU-SeSe. This phenomenon can be attributed to the inevitable oxidation of diselenide bonds during storage. The excellent NO catalytic ability of PCU-SeSe is expected to significantly affect multiple biological behaviors in the blood environment, as shown in the latter sections.

### 3.3. In vitro platelet adhesion

The adhesion of platelet on the surface via non-specific interactions like hydrogen bond and van der Waals forces could cause the treatment failure [40,41]. In particular, the hydrophobicity of the modified sample increased due to the polymer coverage (see Fig. S3 for details). The water

contact angles of PCU-BDO and PCU-SeSe increased significantly. The increase of hydrophobicity may reduce non-specific interactions. Moreover, according to relevant studies [26,36], NO can up-regulate the cGMP level of platelets in the blood environment, thereby inhibiting platelet adhesion, aggregation and activation. As shown in Fig. 4A, serious platelet adhesion and activation can be observed on the 316L surface, either with or without the addition of GSNO. As a comparison, the platelet activation of PCU-BDO decreased significantly due to the polymer covering on the 316L surface. Particularly, PCU-SeSe displayed an even more significant improvement in platelet adhesion with the lowest number of platelets. Meanwhile, in the PCU-SeSe sample containing GSNO, a significant increase of the cGMP concentration can be observed by means of ELISA kit. These results indicate that NO plays a significant role in the anti-adhesion process.

To further quantify the number of platelets adhered to the surfaces, rhodamine was used for fluorescence staining and then the samples were statistically analyzed. As shown in Fig. 4C and D, the platelet adhesion of 316L and PCU-BDO does not change significantly after the addition of GSNO, while that of PCU-SeSe drops significantly. The result is consistent with SEM and cGMP results: 316L and PCU-BDO cannot catalyze the release of NO, while PCU-SeSe can continuously catalyze GSNO and lead to the release of NO, thus significantly protecting the surface from platelet adhesion.

### 3.4. Dynamic hemocompatibility assessment

To test the blood compatibility in real blood flow environment, a dynamic circulation evaluation model [7,12] was constructed using adult New Zealand white rabbits (Fig. 5A). According to the digital photo results (Fig. 5B and C), no detectable occlusion and thrombosis can be observed in the group of the PCU-SeSe sample, while severe occlusion and thrombosis can be observed on the 316L and PCU-BDO. This result was confirmed by SEM images (test samples were obtained from a 15-min circulation assessment) that the PCU-SeSe samples impressively prevented the thrombus formation on their surfaces (Fig. 5D). It can be seen that 316L and PCU-BDO were covered by complex networks of thrombi, while only a tiny number of proteins and blood cells adhere to PCU-SeSe surfaces.

A series of quantitative results were used to analyze the blood compatibility of different samples. Occlusion ratio was obtained by measuring the cross-sectional diameter of the sample catheter. Thrombus weight was calculated by the sample weight difference before and after experiment. Moreover, the sample catheters were injected with simulated body fluid, the time cost was recorded and compared with the initial time to indirectly evaluate the blood flow rate. Among the three samples, it is also shown that the PCU-SeSe sample presents the lowest thrombus weight (2.3 mg, Fig. 5E) as well as the lowest occlusion ratio (9.3%, Fig. 5F); by contrary, it retains the highest blood flow rate (91.3%, Fig. 8G) in the blood flow rates test at the end of circulation. These results strongly indicate that PCU-SeSe has a much better antithrombotic ability than the other surfaces. In general, this novel PCU material in various blood tests exhibited marked inhibition capability of the formation of blood clots.

### 3.5. EC culture

Rapid endothelialization can effectively prevent the occurrence of late thrombosis and restenosis after vascular stent implantation. In order to explore the rapid endothelialization ability of PCU-SeSe, EC adhesion and proliferation experiment *in vitro* were used for relevant investigation. As shown in Fig. 6A and B, fluorescence and counting results of 4 h show that for all the 3 samples, there is no significant difference in the adhesion number of EC either with or without the addition of GSNO. However, 316L showed the largest EC number as the culture time extended to 1 day, which can be attributed to the inherent good cytocompatibility of 316L. Besides, the number of EC on PCU-SeSe surface increased slightly after donor addition compared to that without donor addition. After 3 days of culture, the growth of EC on the surface of PCU-SeSe without GSNO was obviously inferior to that of 316L. Notably, the EC number in PCU-SeSe sample with GSNO increases significantly compared to that without GSNO, indicating that PCU-SeSe can effectively promote EC proliferation in the donor environment. Moreover, the CCK-8 detection results of EC cultured for 1 and 3 days (Fig. 6C) are basically consistent with cell fluorescence and counting results. Although CCK-8 value of PCU-SeSe is inferior to the control sample without GSNO, absorbance of PCU-SeSe is significantly improved after GSNO intervention. These findings suggest that PCU-SeSe in donor environment has excellent endothelial compatibility and is expected to achieve rapid endothelialization in blood vessels.

### 3.6. SMC culture

The proliferation of SMC in vascular pathological region is closely related to intimal hyperplasia. If SMC grows well on the sample surface, the risk of intima hyperplasia may increase after implantation in vascular environment. Therefore, it is necessary to investigate the compatibility of SMC on the modified material surface. As shown in Fig. 7A and B, the fluorescent images and 4 h count shows that PCU-SeSe has the lowest number of SMC adhesion, while the cell adhesion number of PCU-SeSe decreased significantly after GSNO addition. After 1-day culture and 3-

day culture, the SMC skeleton on the surface of PCU-SeSe remains the smallest, in consistency with the CCK-8 detection results. These results indicate that PCU-SeSe could strongly inhibit the growth of SMC in both cell number and cell viability. Such inhibition effect can be further enhanced by the addition of GSNO, which can effectively promote the expression of cGMP in SMC and then inhibit the proliferation of SMC. As can be seen from the cGMP test results (see Supplementary Fig. S4), only the cGMP level of PCU-SeSe is significantly improved after GSNO addition. Therefore, it can be concluded that PCU-SeSe has a strong inhibitory effect on the proliferation of SMC in blood vessels.

### 3.7. Subcutaneous implantation

When the materials are implanted into the subcutaneous tissue of animals, different thicknesses of fibrous capsules will be generated, and the fibrous capsules can be used to evaluate the degree of inflammation after implantation [14,23]. The main purpose of this experiment is to explore the anti-inflammatory ability of PCU-SeSe coating in the non-donor environment. Here, SD rats were selected for subcutaneous implantation in this study. As shown in Fig. 8, the fibrous capsules of the 3-week PCU-SeSe samples are the thinnest with only  $21.1 \pm 1.4 \mu\text{m}$ , indicating the weakest inflammatory response among different samples. With the extension of implantation time (9 weeks), fibrous capsules tend to be more mature. Nevertheless, PCU-SeSe still maintains the weakest inflammatory response with a fibrous capsules thickness of  $32.1 \pm 2.5 \mu\text{m}$ . As a comparison, the fibrous thickness of 316L and PCU-BDO is increased to a much higher value of  $119.1 \pm 17.3$  and  $90.2 \pm 5.4 \mu\text{m}$  respectively. These results are consistent with MA culture (see Fig. S5 for details) and inflammatory factor release *in vitro* (see Fig. S6 for details), suggesting that PCU-SeSe possesses excellent anti-inflammatory activity. The MA growth was inhibited on PCU-SeSe surfaces, especially after adding NO donor. Moreover, the release of inflammatory factor including TNF- $\alpha$  and IL-6 also be suppressed. Thereout, combined with other cell results, this novel PCU material showed well EC compatibility after adding NO donor, while it could significantly suppress the proliferation of SMC and MA.

### 3.8. Wire and endovascular stent implantation

When the device was implanted into the blood vessel, both SMC and EC will migrate and grow to the device surface, thus forming new vascular tissue. In this process, the new vascular tissue can be used to evaluate the biological behavior of the implant material, and then determine the potentiality as the intravascular stent. As shown in the implant diagram (Fig. 9A), new tissues would be formed on the samples surface after 30 days of indwelling in the vessels. SEM results (Fig. 9B) show that the long axis direction of the cells on PCU-SeSe surface was consistent with the direction of blood flow, and almost no blood cells could be observed. Meanwhile, obvious blood cells adhesion and aggregation could be observed on the regenerated tissue surface of 316L. These results suggested that PCU-SeSe is superior to 316L in promoting healthy endothelialization and thrombotic inhibition. Much better ability to inhibit hyperplasia is also observed in PCU-SeSe in subsequent HE staining (Fig. 9B). Compared with 316L ( $69.7 \pm 8.9 \mu\text{m}$ ), the thickness of regenerated tissue on PCU-SeSe surface is much thinner ( $37.2 \pm 3.4 \mu\text{m}$ ). This phenomenon can be associated with the inhibition of SMC proliferation by PCU-SeSe material. Moreover, SMC and MA in the regenerated tissues were specifically labeled by immunofluorescence for further analysis. On the one hand, the expression level of CD 206 (M2-type MA) of 316L was markedly lower than that of PCU-SeSe (Fig. S7A), indicating that the anti-inflammatory level of 316L was insufficient. On the other hand, the expression level of OPN was higher than that of  $\alpha$ -SMA for 316L (see Fig. S7B for details), which means a higher risk of endometrial hyperplasia. In contrast, PCU-SeSe exhibited lower OPN expression. The results of immunofluorescence double staining showed that 316L modified by PCU-SeSe could significantly affect the SMC type of regenerated

tissue.

To investigate the biological behaviors of PCU-SeSe applied to long-term indwelling devices, PCU-SeSe was coated on the vascular stent surface and then implanted into the iliac artery of rabbit. After 30 days, the stents together with the surrounding blood vessels were harvested and then used for neointima observations and tissue section. It can be seen from SEM images (Fig. 9C) that many parts of the 316L stent surface were already covered by neointima, but still some parts remain uncovered. Besides, a large number of red blood cells, platelets and other blood components can be observed on the surface. By contrary, the stent surface modified by PCU-SeSe is thoroughly covered and only a small amount of blood cell can be observed. The uncovered part of bare-metal stents and significant blood cell adhesion put 316L stent at significant risk for late thrombosis. In addition to the threat of late thrombosis, restenosis is also a pain point in the clinical application of stents. After the hard tissue embedding of neointimal, the resulting samples were used for sectioning and microscopy. By comparing the histological pictures (Fig. 9C), it can be seen that the hyperplasia thickness of the 316L stent covered by the neointima is markedly larger than that of the PCU-SeSe sample. These results correspond to the results of HE staining and immunofluorescence staining of the abdominal aorta implantation, indicating that PCU-SeSe can effectively prevent intima hyperplasia after implantation. In summary, animal experiments further indicated that this novel material is believed to create a favorable condition of inhibiting inflammation, healthy endothelialization, combating thrombus and reducing restenosis.

#### 4. Conclusion

In summary, selenium-functionalized polycarbonate-polyurethane i.e., PCU-SeSe, was synthesized for surface modification of blood-contacting devices with the GPx mimics catalytic capability. The dynamic diselenide bond allows PCU-SeSe coating to catalyze the release of NO continuously and controllably in the donor environment, which endows the PCU-SeSe with multiple functions in blood environment. A series of experiments validate that the PCU-SeSe coating exhibits excellent antithrombosis, anti-cell adhesion and EC compatibility. Moreover, animal experiments *in vivo* further indicate that PCU-SeSe coating on vascular stent surface could create a favorable condition for inhibiting inflammation, healthy endothelialization, anti-thrombogenesis and restenosis prevention. It is expected that this novel PCU-based material could open up a new avenue for functionalizing blood-contacting devices and bring new enlightenment to other clinical implants.

#### CRediT authorship contribution statement

**Peichuang Li:** Conceptualization, Data curation, Formal analysis, Investigation, Methodology, Resources, Software, Supervision, Validation, Visualization, Writing – original draft, Writing – review & editing. **Wanhao Cai:** Formal analysis, Methodology, Software, Supervision, Writing – original draft, Writing – review & editing. **Kebing Wang:** Methodology. **Lei Zhou:** Methodology. **Shusheng Tang:** Methodology. **Yuancong Zhao:** Conceptualization, Data curation, Formal analysis, Funding acquisition, Investigation, Methodology, Project administration, Supervision, Validation, Visualization. **Xin Li:** Data curation, Formal analysis, Investigation, Methodology, Project administration, Supervision, Validation, Visualization. **Jin Wang:** Conceptualization, Data curation, Formal analysis, Funding acquisition, Investigation, Methodology, Project administration, Supervision, Validation, Visualization.

#### Declaration of competing interest

The authors declare that they have no known competing financial interests or personal relationships that could have appeared to influence the work reported in this paper.

#### Acknowledgements

This work was financially supported by Natural Science Foundation of China (NSFC Project 32071328 & 81801853), Sichuan Science and Technology Program (2019YFH049 & 2020YFH0103), and Fundamental Research Funds for the Central Universities (LKP2020-L).

#### Appendix A. Supplementary data

Supplementary data to this article can be found online at <https://doi.org/10.1016/j.smain.2022.04.003>.

#### References

- [1] L. Li, L. Yang, Y. Liao, H. Yu, Z. Liang, B. Zhang, et al., Superhydrophilic versus normal polydopamine coating: a superior and robust platform for synergistic antibacterial and antithrombotic properties, *Chem. Eng. J.* 402 (2020), 126196.
- [2] B. O'Brien, W. Carroll, The evolution of cardiovascular stent materials and surfaces in response to clinical drivers: a review, *Acta Biomater.* 5 (2009) 945–958.
- [3] K. Suemitsu, O. Iida, T. Shiraki, S. Suemitsu, M. Murakami, M. Miyamoto, et al., Predicting loss of patency after forearm loop arteriovenous graft, *J. Vasc. Surg.* 64 (2016) 395–401.
- [4] H. Kawakami, Polymeric membrane materials for artificial organs, *J. Artif. Organs* 11 (2008) 177–181.
- [5] P. Ravani, R. Quinn, M. Oliver, B. Robinson, R. Pisoni, N. Pannu, et al., Examining the association between hemodialysis access type and mortality: the role of access complications, *Clin. J. Am. Soc. Nephrol.* 12 (2017) 955–964.
- [6] T. Yang, Z. Du, H. Qiu, P. Gao, X. Zhao, H. Wang, et al., From surface to bulk modification: plasma polymerization of amine-bearing coating by synergic strategy of biomolecule grafting and nitric oxide loading, *Bioact. Mater.* 5 (2020) 17–25.
- [7] H. Qiu, Q. Tu, P. Gao, X. Li, M.F. Maitz, K. Xiong, et al., Phenolic-Amine chemistry mediated synergistic modification with polyphenols and thrombin inhibitor for combating the thrombosis and inflammation of cardiovascular stents, *Biomaterials* 269 (2021) 120626.
- [8] S. Unterman, A. Freiman, M. Beckerman, E. Abraham, J.R. Stanley, E. Levy, et al., Tuning of collagen scaffold properties modulates embedded endothelial cell regulatory phenotype in repair of vascular injuries *in vivo*, *Adv. Healthc. Mater.* 4 (2015) 2220–2228.
- [9] L. Yang, H. Wu, Y. Liu, Q. Xia, Y. Yang, N. Chen, et al., A robust mussel-inspired zwitterionic coating on biodegradable poly (L-lactide) stent with enhanced anticoagulant, anti-inflammatory, and anti-hyperplasia properties, *Chem. Eng. J.* 427 (2022), 130910.
- [10] T. Zhu, W. Gao, D. Fang, Z. Liu, G. Wu, M. Zhou, et al., Bifunctional polymer brush-grafted coronary stent for anticoagulation and endothelialization, *Mater. Sci. Eng. C* 120 (2021), 111725.
- [11] J. Li, S. Wang, Y. Sheng, C. Liu, Z. Xue, P. Tong, et al., Designing HA/PEI nanoparticle composite coating on biodegradable Mg-Zn-Y-Nd alloy to direct cardiovascular cells fate, *Smart Mater. Med.* 2 (2021) 124–133.
- [12] H. Yu, H. Qiu, W. Ma, M.F. Maitz, Q. Tu, K. Xiong, et al., Endothelium-Mimicking surface combats thrombosis and biofouling via synergistic long-and short-distance defense strategy, *Small* (2021), 2100729.
- [13] Y. Yu, S.-J. Zhu, H.-T. Dong, X.-Q. Zhang, J.-A. Li, S.-K. Guan, A novel MgF<sub>2</sub>/PDA/SH-A coating on the bio-degradable ZE21B alloy for better multi-functions on cardiovascular application, *J. Magnes. Alloys* (2021), <https://doi.org/10.1016/j.jma.2021.06.015>.
- [14] K. Wang, T. Shang, L. Zhang, L. Zhou, C. Liu, Y. Fu, et al., Application of a reactive oxygen species-responsive drug-eluting coating for surface modification of vascular stents, *ACS Appl. Mater. Interfaces* 13 (2021) 35431–35443.
- [15] J. Li, W. Li, D. Zou, F. Kou, Y. Hou, A. Yasin, et al., Comparison of conjugating chondroitin sulfate A and B on amine-rich surface: for deeper understanding on directing cardiovascular cells fate, *Compos. B Eng.* 228 (2022), 109430.
- [16] J. Chen, P. Yang, Y. Liao, J. Wang, H. Chen, H. Sun, et al., Effect of the duration of UV irradiation on the anticoagulant properties of titanium dioxide films, *ACS Appl. Mater. Interfaces* 7 (2015) 4423–4432.
- [17] B. Qu, L. Yuan, L. Yang, J. Li, H. Lv, X. Yang, Polyurethane end-capped by tetramethylpyrazine-nitrone for promoting endothelialization under oxidative stress, *Adv. Healthc. Mater.* 8 (2019), 1900582.
- [18] A.A. Gostev, A.A. Karpenko, P.P. Laktionov, Polyurethanes in cardiovascular prosthetics, *Polym. Bull.* 75 (2018) 4311–4325.
- [19] C. Lu, N. Zhou, D. Xu, Y. Tang, S. Jin, Y. Wu, et al., Surface-initiated reverse atom transfer radical polymerization (SI-RATRP) for blood-compatible polyurethane substrates, *Appl. Surf. Sci.* 258 (2011) 618–626.
- [20] A.-C. Strömdahl, L. Ignatowicz, G. Petruk, M. Butrym, S. Wasserstrom, A. Schmidtchen, et al., Peptide-coated polyurethane material reduces wound infection and inflammation, *Acta Biomater.* 128 (2021) 314–331.
- [21] C. Xu, A.E. Kuriakose, D. Truong, P. Punnakitkashem, K.T. Nguyen, Y. Hong, Enhancing anti-thrombogenicity of biodegradable polyurethanes through drug molecule incorporation, *J. Mater. Chem. B* 6 (2018) 7288–7297.
- [22] L.-C. Xu, M.E. Meyerhoff, C.A. Siedlecki, Blood coagulation response and bacterial adhesion to biomimetic polyurethane biomaterials prepared with surface texturing and nitric oxide release, *Acta Biomater.* 84 (2019) 77–87.

- [23] P. Li, W. Cai, X. Li, K. Wang, L. Zhou, T. You, et al., Preparation of phospholipid-based polycarbonate urethanes for potential applications of blood-contacting implants, *Regen. Biomater.* 7 (2020) 491–504.
- [24] J.J. Wykrzykowska, Y. Onuma, P.W. Serruys, Advances in stent drug delivery: the future is in bioabsorbable stents, *Expert Opin. Drug Deliv.* 6 (2009) 113–126.
- [25] A.W. Carpenter, M.H. Schoenfisch, Nitric oxide release: Part II. Therapeutic applications, *Chem. Soc. Rev.* 41 (2012) 3742–3752.
- [26] P.N. Coneski, M.H. Schoenfisch, Nitric oxide release: Part III. Measurement and reporting, *Chem. Soc. Rev.* 41 (2012) 3753–3758.
- [27] F. Zhang, Q. Zhang, X. Li, N. Huang, X. Zhao, Z. Yang, Mussel-inspired dopamine-CuII coatings for sustained in situ generation of nitric oxide for prevention of stent thrombosis and restenosis, *Biomaterials* 194 (2019) 117–129.
- [28] Y. Yang, P. Gao, J. Wang, Q. Tu, L. Bai, K. Xiong, et al., Endothelium-mimicking multifunctional coating modified cardiovascular stents via a stepwise metal-catechol-(amine) surface engineering strategy, *Research* 2020 (2020), 9203906.
- [29] Z. Yang, Y. Yang, K. Xiong, X. Li, P. Qi, Q. Tu, et al., Nitric oxide producing coating mimicking endothelium function for multifunctional vascular stents, *Biomaterials* 63 (2015) 80–92.
- [30] T. Yang, A.N. Zelikin, R. Chandrawati, Progress and promise of nitric oxide-releasing platforms, *Adv. Sci.* 5 (2018), 1701043.
- [31] C.W. McCarthy, R.J. Guillory, J. Goldman, M.C. Frost, Transition-metal-mediated release of nitric oxide (NO) from S-nitroso-N-acetyl-d-penicillamine (SNAP): potential applications for endogenous release of NO at the surface of stents via corrosion products, *ACS Appl. Mater. Interfaces* 8 (2016) 10128–10135.
- [32] R.J. Singh, N. Hogg, J. Joseph, B. Kalyanaraman, Mechanism of nitric oxide release from S-nitrosothiols, *J. Biol. Chem.* 271 (1996) 18596–18603.
- [33] W. Cha, M.E. Meyerhoff, Catalytic generation of nitric oxide from S-nitrosothiols using immobilized organoselenium species, *Biomaterials* 28 (2007) 19–27.
- [34] C. Liu, J. Xia, S. Ji, Z. Fan, H. Xu, Visible-light-induced metathesis reaction between diselenide and ditelluride, *Chem. Commun.* 55 (2019) 2813–2816.
- [35] N. Ma, Y. Li, H. Xu, Z. Wang, X. Zhang, Dual redox responsive assemblies formed from diselenide block copolymers, *J. Am. Chem. Soc.* 132 (2010) 442–443.
- [36] Y. Fan, Y. Zhang, Q. Zhao, Y. Xie, R. Luo, P. Yang, et al., Immobilization of nano Cu-MOFs with polydopamine coating for adaptable gasotransmitter generation and copper ion delivery on cardiovascular stents, *Biomaterials* 204 (2019) 36–45.
- [37] B. Lu, X. Han, A. Zhao, D. Luo, M.F. Maitz, H. Wang, et al., Intelligent H<sub>2</sub>S release coating for regulating vascular remodeling, *Bioact. Mater.* 6 (2021) 1040–1050.
- [38] S. Ji, W. Cao, Y. Yu, H. Xu, Dynamic diselenide bonds: exchange reaction induced by visible light without catalysis, *Angew. Chem. Int. Ed.* 53 (2014) 6781–6785.
- [39] F. Fan, S. Ji, C. Sun, C. Liu, Y. Yu, Y. Fu, et al., Wavelength-controlled dynamic metathesis: a light-driven exchange reaction between disulfide and diselenide bonds, *Angew. Chem. Int. Ed.* 57 (2018) 16426–16430.
- [40] W. Cai, C. Xiao, L. Qian, S. Cui, Detecting van der Waals forces between a single polymer repeating unit and a solid surface in high vacuum, *Nano Res.* 12 (2019) 57–61.
- [41] W. Cai, D. Xu, F. Zhang, J. Wei, S. Lu, L. Qian, et al., Intramolecular hydrogen bonds in a single macromolecule: strength in high vacuum versus liquid environments, *Nano Res.* 15 (2022) 1517–1523.